Supplementary Information

S1 Modelling pressure and flow dynamics

Air flow to the SPA is generated by the pneumatic supply system as shown in Fig. 1A, commonly consisting of a *source* that generates the pressurized air, a *valve*, that controls the direction of flow, and *pneumatic line* that enables air flow between the different components[31]. We first apply the following assumptions[39]: (i) air behaves as an ideal gas, (ii) the ambient is at standard pressure, $P_0 =$ 100 kPa (absolute pressure), and temperature , $T_0 = 293.15$ K; (iii) all processes are isothermal, occurring at T_0; and (iv) air pressure is uniform inside the SPA. Using the ideal gas law, the SPA pressure dynamics can be expressed as[31]:

$$\frac{d}{dt}(P_{spa}V_{spa}) = P_0 Q_{spa} \tag{S1}$$

where P_{spa} and V_{spa} are the instantaneous SPA pressure and volume respectively, and Q_{spa} is the mass flow rate expressed as volumetric flow at standard conditions, $P_0 = 100$ kPa (absolute pressure), $T_0 = 293$ K. Integrating between initial time, t_0, and current time, t, and rearranging, we get,

$$[P_{spa}V_{spa}]_t = P_0 \int_{t_0}^{t} Q_{spa}dt + [P_{spa}V_{spa}]_{t_0} \tag{S2}$$

where $[P_{spa}]_{t_0}$ is simply equal to P_0 and $[V_{spa}]_{t_0}$ is equal to the deflated SPA volume = 83mL.

From the above, SPA instantaneous volume can be calculated as:

$$[V_{spa}]_t = \frac{[P_{spa}V_{spa}]_t}{[P_{spa}]_t} \tag{S3}$$

Q_{spa} can be measured directly through the use of flow sensors. Alternatively, we can also model and estimate it in real-time as it is governed by the source and SPA pressures[31,39] and valve state. Here, we model it using the ISO 6358 standards[40] as,

$$Q_{spa} = C\Psi P_{High} \tag{S4}$$

$$\Psi = \begin{cases} \left[1 - \left(\frac{\frac{P_{Low}}{P_{High}} - b}{1-b}\right)^2\right]^m, & \frac{P_{Low}}{P_{High}} \geq b \\ 1, & \frac{P_{Low}}{P_{High}} < b \end{cases} \tag{S5}$$

where, C, b, and m are the sonic conductance, critical ratio ($0 < b < 1$) and the subsonic index ($0 < m < 1$), respectively; P_{High} and P_{Low} are the absolute upstream and downstream pressures respectively; and Ψ is the non-linear flow function. During inflation, $P_{High} = P_{src}$, and $P_{Low} = P_{spa}$. During deflation, $P_{High} = P_{spa}$, and $P_{Low} = P_0$. The above expression can be used to calculate the flow through a PSS consisting of a wide range of pneumatic components including valves, tubing and fittings[31,39].

To find the ISO 6358 parameters of C, b, and m, for our experimental setup, we inflated and deflated the SPA-pack cyclically between 0 kPa to 200 kPa ten times, measured the pressure and flow (Fig. S1), and fitted the parameters of (S4) and (S5) to the measured data, using the *lsqcurvefit* solver in MATLAB. Fig. S1C shows the measured vs. modelled flow. Table S1 shows the fitted values of the ISO 6358 model for the flow paths of inflation and deflation.

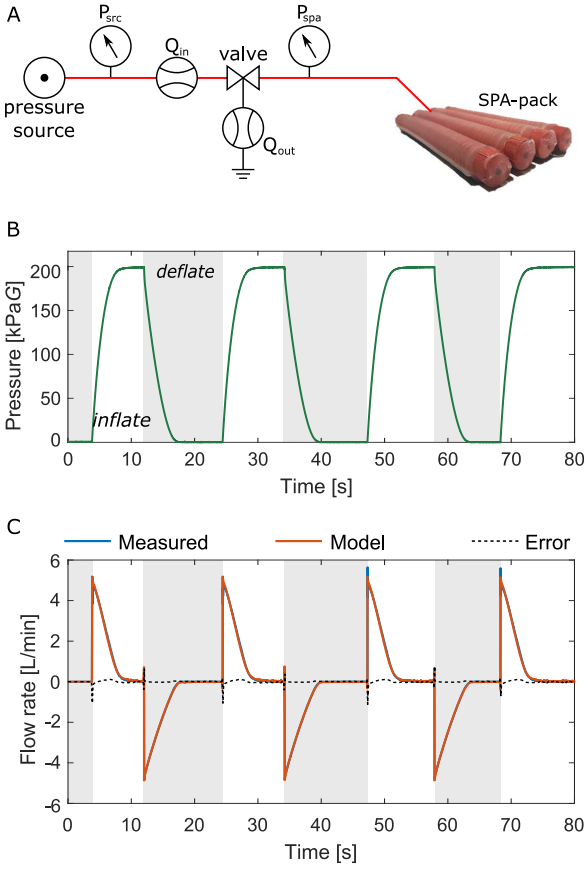

Fig. S1 PSS characterization: We powered an SPA-pack[32] using a PSS, measured the flow during inflation and deflation, and fit the model parameters C_{eq}, b_{eq}, and m_{eq} to the measured data. (A) The SPA-pack used for testing, (B) The measured pressure response depicting inflation and deflation regions, (C) Measured vs. calculated flow using ISO 6358[40].

Table S1 ISO 6358 parameters for Inflation and deflation

Valve path	C [lpm/kPa]	b	m
Inflation	1.8×10^{-2}	0.15	0.57
Deflation	1.74×10^{-2}	0.12	0.6

S2 Calculating ground-truth values for displacement in Three-point bending

For three point bending, we enforce the anchoring condition by securing the central section of the SPA-pack in a cantilever constraint on module 2 of the robotic platform, and enveloping an overlapping fabric as shown in Fig. 3B. During testing, we measure the force F_y recorded by the load-cell of module 2 as shown in Fig. 2. The displacement is defined by the deflection of the SPA mid-point with respect to its two ends, which we enforced by controlling the linear motor of module 2. As the SPA is constrained between the linear motor and the fabric straps, the SPA displacement is equal

to that of the linear motor only when the strap is taught. When the strap is loose, the SPA is unconstrained, i.e. in free expansion, and hence, the displacement of the linear motor is not equal to that of the SPA. Rather than using external sensors for calculating displacement, we calculated the SPA displacement using the existing setup.

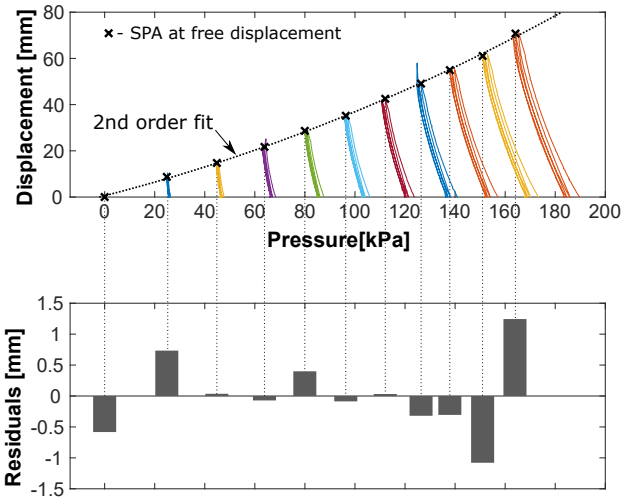

Fig. S2 Defining displacement of the SPA-pack for three-point bending. We first separated the regions for constrained and free expansion, and plotted the pressure vs. displacement of the SPA-pack in the constrained expansion region. The points of largest displacement then correspond to the initiation of free expansion. We noted these points for the *hold* loading sequence, and fitted a second order polynomial to define the displacement as a function of SPA pressure. Good agreement is seen between the model and measured values as observed from the residuals.

First, we identified whether the SPA is constrained or unconstrained, using a small threshold on the measured force, $F_{min} = 1N$. For the constrained region ($F > F_{min}$), we considered displacement equal to that of the linear motor. For the unconstrained condition ($F < F_{min}$), as the displacement is only governed by the SPA air pressure, we modelled the free displacement as a function of its pressure. To find this mapping, we first plotted the measured pressure vs. *module 2* displacement in the constrained region ($F > F_{min}$), for the *hold* loading sequence. Then, we marked the points with largest displacement as shown in Fig. S2. These points correspond to the instances when the strap tension just becomes zero, thereby corresponding to the boundary between constrained and unconstrained SPA displacement. Using these points, we fitted a second order polynomial, as shown by the dotted curve in Fig. S2. Using this method, we identified regions of constrained and unconstrained displacement in the entire dataset, and calculated the displacement for the SPA-pack.

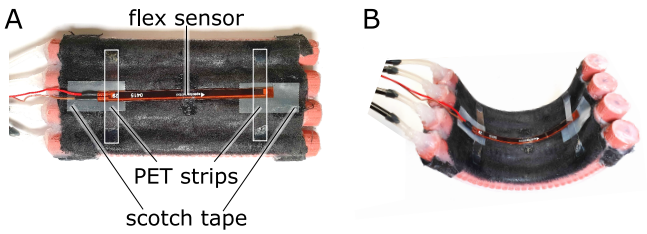

Fig. S3 The SPA-pack sensorized with a standard flex sensor. We affixed a standard flex sensor (SpectraSymbol, 113mm x 6.4mm x 0.5mm) on the non-extending side of the SPA-pack. We affixed it at the centre only using silicone glue, Dow Corning 734. Additionally, we secured two PET strips on the SPA, which prevent the ends of the flex sensor from bending outwards from the SPA. Lastly, we stuck a low-friction tape between the flex sensor and the SPA-pack, which allowed the ends of the flex sensor to glide freely over the SPA-pack during bending. A. The SPA-pack in deflated state, B. The SPA-pack in inflated state.

Table S2 Errors and coefficients of determination for bijective mapping for pulling

Mapping	rms errors	R^2
$P_{spa}, V_{spa} \rightarrow F$	1.90N	0.88
$P_{spa}, V_{spa} \rightarrow x$	5.44mm	0.96
$P_{spa}, x \rightarrow V_{spa}$	0.18mL	>0.99

Table S3 Errors and coefficients of determination for bijective mapping for three-point bending

Mapping	rms errors	R^2
$P_{spa}, V_{spa} \rightarrow F$	2.57N	0.94
$P_{spa}, V_{spa} \rightarrow x$	1.49mm	0.98
$P_{spa}, x \rightarrow V_{spa}$	0.1782mL	>0.99